7. Gregory C.A., Luis F.S. Kv2 channels oppose myogenic constriction of rat cerebral arteries // Am. J. Physiol. Cell. Physiol. 2006. Vol. 291, No. 2. P. C348–C356.
8. Harm J.K., Mark T.N. Regulation of arterial diameter and wall [Ca^{2+}] in cerebral arteries of rat by membrane potential and intravascular pressure // J. Physiol. 1998. Vol. 508. P. 199–209.
9. Lopez-Barneo J., Lopez-Lopez J.R., Urena J., Gonzalez C. Chemotransduction in the carotid body: K+ current modulated by PO_2 in type-chemoreceptor cells // Science. 1988. Vol. 241 (4865). P. 580–582.
10. Siesjö B.K. Pathophysiology and treatment of focal cerebral ischemia. Part II: Mechanisms of damage and treatment // J. Neurosurg. 1992. Vol. 77, No. 3. P. 337–354.
11. Standen N.B., Quayle J.M. K^+ channel modulation in arterial smooth muscle // Acta Physiol. Scand. 1998. Vol. 164, No. 4. P. 549–557.
12. Uski T.K., Hogestatt E.D. Effects of various cyclooxygenase and lipoxygenase metabolites on guinea-pig cerebral arteries // Gen. Pharmacol. 1992. Vol. 23, No. 1. P. 109–113.
13. Zhu D., Medhora M., Campbell W.B. et al. Chronic hypoxia activates lung 15-lipoxygenase, which catalyzes production of 15-HETE and enhances constriction in neonatal rabbit pulmonary arteries // Circ. Res. 2003. Vol. 92, No. 9. P. 992–1000.
14. Zhu Y., Shan H., Li Q., Zhu D. Contractile effect and mechanism of 15-HETE on hypoxic rat internal carotid arteries rings // Chinese Pharmacological Bulletin. 2005. Vol. 21, No. 11. P. 1327–1332.
15. Zhu Yu-Lan, Su Fang, Chan He, Zhu Da-1ing. Expression and location of 15-lipoxygenase in hypoxic rat brain // Journal of Clinical Rehabilitative Tissue Engineering Research. 2005. Vol. 9, No. 1. P. 90–92.

Поступила в редакцию 24.06.2013.

РОЛЬ 15-ГИДРОКСИЭЙКОЗАТЕТРАЕНОВОЙ КИСЛОТЫ В ИНАКТИВАЦИИ КАЛИЕВЫХ КАНАЛОВ И СПАЗМЕ ВНУТРЕННЕЙ СОННОЙ АРТЕРИИ ПРИ ГИПОКСИИ

Янмей Жу[1], Ли Чен[1], Веньян Лиу[1], Вейжи Ванг[1], Далинг Жу[2], Юлан Жу[1]

[1] *Второй аффилированный госпиталь,* [2] *Фармацевтический колледж Харбинского медицинского университета (КНР, 150081, г. Харбин, р-н Наньган, шоссе Баоян, 157)*

Тяжелая гипоксия вызывает спазм внутренней сонной артерии, который опасен ишемическим повреждением головного мозга. Некоторые метаболиты могут спровоцировать вазоконстрикцию, однако механизм их действия до конца не расшифрован. В эксперименте на крысах исследовали влияние 15-гидроксиэйкозатетраеновой кислоты (15-HETE), продуцируемой 15-липоксигеназой, на тонус сосудов при гипоксии. Обнаружено повышение уровня 15-липоксигеназы в эндотелии и гладкомышечных клетках внутренней сонной артерии. 15-HETE обусловливала дозозависимый спазм сосуда, а также снижение активности потенциалзависимых калиевых каналов. Таким образом, инактивация калиевых каналов 15-HETE при гипоксии приводит к ослаблению реполяризации активных потенциалов и притоку калия в клетки, что вызывает повышение тонуса гладкой мускулатуры сосудов и спазм внутренней сонной артерии.

Ключевые слова: *потенциалзависимые калиевые каналы, гладкомышечные клетки, церебральный вазоспазм.*

Pacific Medical Journal, 2013, No. 4, p. 63–67.

УДК 616-006.484-085277.3:615.831

THE INHIBITING EFFECT OF PHOTODYNAMIC THERAPY AND NOVEL RECOMBINANT HUMAN ENDOSTATIN ON THE *IN VIVO* GROWTH OF U251 HUMAN GLIOMA XENOGRAFTS

Hu Shaoshan[1], *Zhan Qi*[2], *Yue Wu*[2]

[1] Second Affiliated Hospital, [2] Fourth Affiliated Hospital of Harbin Medical University (157 Baojian Road, Nangang District, Harbin 150081 P.R. China)

Keywords: *malignant tumors, endostar, hypoxia inducible factor, vascular endothelial growth factor.*

Summary – Endostar, a novel recombinant human endostatin expressed in Escherichia coli, was approved by the State FDA in China. To investigate the effect of endostar and photodynamic therapy (PDT) on the in vivo growth of U251 glioma. Seven days after inoculation with U251 cells, nude mice with MRI-confirmed glioma were randomly assigned to 4 groups: PDT+endostar group; PDT group; endostar group and control group. In the PDT group, survival prolonged, accompanied by an increase in apoptosis, when compared with the control group. Furthermore, these changes were more pronounced in the PDT+endostar group. After PDT, hypoxia inducible factor-1α (HIF-1α) and vascular endothelial growth factor A (VEGF-A) expression was markedly increased and after endostar treatment, HIF-1α and VEGF-A expression was significantly reduced. PDT, in combination with endostar, can significantly inhibit the growth of U251 glioma. This approach may represent a promising strategy in the treatment of malignant tumors.

Glioma is a common intracranial malignancy accounting for approximately 40–50 % of intracranial malignancies. The 5-year survival rate is approximately 30 % in patients with astrocytoma [14]. Photodynamic therapy (PDT) has been an effective auxiliary strategy in the treatment of glioma [11]. PDT treatment is based on the presence of a drug with photosensitizing properties combined with visible or far red light and oxygen.

Following PDT, a state of hypoxia is induced within the tumor tissue as a result of rapid oxygen consumption [4]. Tissue hypoxia induces a plethora of molecular and physiological responses, including an adaptive response associated with gene activation. A primary step in hypoxia-mediated gene activation is the formation of the transcription factor complex (hypoxia inducible factor-1 – HIF-1). A number of HIF-1-responsive genes have been identified, including vascular endothelial growth factor (VEGF), erythropoietin, and glucose transporter-1. VEGF, also called vascular permeability factor, is an endothelial cell-specific mitogen involved in the induction and maintenance of the neovasculature in solid tumors [7].

A. Ferrario et al. [5] applied PDT in the treatment of mouse breast cancer. The results showed that HIF-1α and VEGF expression was increased after PDT but was markedly decreased after treatment with angiogenesis inhibitors (IM862 and EMAP-2). R. Bhuvaneswari et al. [2] revealed that subcurative PDT in an orthotopic model of prostate cancer increases not only VEGF secretion but also the fraction of animals with lymph node metastases. PDT followed

Shaoshan Hu – postdoctor, professor of Harbin Medical University; e-mail: shaoshanhu@hotmail.com

by administration of an antiangiogenic agent, TNP-470, abolished this increase and reduced local tumor growth. Q. Zhou et al. [15] applied PDT in the treatment of mouse nasopharyngeal carcinoma. The semiquantitative RT-PCR results showed that the expression of HIF-1α and VEGF were increased in PDT-treated tumor samples collected 24 h post-PDT. SU5416 and SU6668 in combination with PDT, when used in the treatment, not only prolonged mouse survival but also inhibited cancer growth.

To sum up, in addition to an incomplete tumor cell kill, the ultimate failure of PDT as a treatment of cancer, might be attributed to enhanced angiogenesis powered by PDT induction of VEGF. PDT induction of VEGF could lead to angiogenesis which is associated with tumor growth and metastasis, therefore mitigating its cytotoxic and antivascular effects.

Endostar, a novel recombinant human endostatin expressed in Escherichia coli, was approved by the State FDA in China. Studies have reported that these antiangiogenic effect of endostatin were related with VEGF, which is a crucial regulator in angiogenesis.

In the present study, the effect of hematoporphyrin monomethyl ether mediated PDT and endostar on the growth of glioma was investigated in order to explore their anti-angiogenesis effect on glioma. We also studied HIF-1α and VEGF-A expression to better understand the mechanism of action of PDT on glioma with the hope that our results may demonstrate the clinical application of PDT.

Methods

The U251 glioma cell line was purchased from the Beijing Institute of Science, and cultured in RPMI 1640 medium containing 10 % fetal bovine serum in an incubator containing 5 % CO_2 at 37 °C.

BALB/c (nu/nu) nude mice weighing 20–22 g (specific pathogen free; Beijing Vitalriver Experimental Animal Co., Ltd; License No. 021). Implantation technique of U251 cells were performed, as in previous studies [3]. Nude mice were anaesthetized with 5 mg/kg xylazine and then fixed in a stereotaxic instrument. After sterilization and skin incision, a hole was made on the skull at 1.0 mm anterior to the anterior fontanel, 2.0 mm lateral to the sagittal suture. The needle of a 50 μl microsyringe (Hamilton, Bonaduz, Switzerland) was inserted to a 3mm beneath dura through the center of the skull hole and 5×105 U251 cell in 3 μl PBS were injected intracerebrally during a 5 min interval and the syringe remained in the brain for 5 min followed by slow retraction. The hole was sealed with bone wax and the wound was closed.

Magnetic resonance imaging (MRI) scanning was carried out using the Signa 3.0 T MR System. The conditions for scanning were performed as previously described [10]: T1WI and T2WI coronal and horizontal images were acquired from both unenhanced and enhanced scans. Scanning parameters were slice thickness 3 mm, interval 0.3 mm, FOV 8×8 cm, matrix 196×160, 2 NEX. T1WI: SE array, TR450, TE8.6, SL: 3mm. T2WI: TR5020, TE100, SL: 3mm.For enhanced scan, Gd-DTPA (Schering AG , Germany, 0.2 mmol/kg) was injected peritoneally. The largest enhancing areas in the horizontal and coronal planes were analyzed and the maximum anteroposterior diameter (L), width (W) and height (H) determined were used for the calculation of tumor volume (V), as follows:

$$V = (4/3 \times \pi \times L \times W \times H) \times 1/8 \ (mm^3).$$

One week after inoculation, MRI was employed to detect cancer in the brains of the rats. A total of 60 male nude mice with glioma were randomly assigned into 4 groups (n=15 per group): PDT+endostar group, PDT group, endostar group and control group. Eight days after inoculation, PDT was carried out and 0.5 ml of endostar (corporation of Simcere, Nanjing, China; Concentration: 5 mg/ml; doses 20 mg/kg) was given every day intraperitoneal injection for 14 days, as in previous studies [9]. Nude mice in the control group and the PDT group received equivalentnormal saline. On day 21, 5 nude mice in each group were sacrificed followed by transcardial perfusion with 4 % paraformaldehyde and gliomas were surgically removed using a microsurgical technique. The tumor was harvested for immunohistochemistry and ELISA. The remaining 10 nude mice in each group were used to determine survival rates. MRI was performed at 3 weeks after inoculation to detect tumor volume . All experimental procedures were approved by the Institutional Animal Care and Use Committee. Gliomas were surgically removed using a microsurgical technique.

PDT was carried out, as previously described [8]. HMME (Fudan Zhangjiang Biotech Co., Ltd, CHINA; 5 mg/kg) was injected peritoneally, and 3 h later animals were anesthetized with 10 % chloral hydrate and fixed in a stereotaxic device, the skull was exposed, and a 1 mm diameter craniotomy was drilled over the right hemisphere 2.5 mm to the midline and 2.0 mm anterior to the bregma. Three minutes later, the inoculated tumor was exposed with microneurosurgical method. The optical fiber of the PDT instrument (DIOMED 630 Limited , British , wavelength: 630 nm) was placed on the tumor followed by photodynamic treatment for 10 min. The treatment dose rates were 120 J/cm2. After PDT, the hole was sealed with bone wax and skin was sutured. Nude mice in the antibody group and the control group did not receive HMME, but were administered all other procedures.

Tissues were embedded in paraffin and cut into 5-μm sections followed by hematoxylin and eosin staining. Sections were observed under a light microscope. For immunohistochemistry, sections were deparaffinized and hydrated followed by antigen retrieval. Endogenous peroxidase was inactivated with hydrogen peroxide. These sections were treated with rabbit anti-human HIF-1α antibody (1:200) or with rabbit anti-human VEGF-A antibody (1:100); rabbit anti-human GFAP antibody (1:200). Immunohistochemistry was performed according to the manufacturer's instructions. Evaluation of sections was performed based on the proportion of positive cells: <10 %, negative (–); 11–30 %, weakly positive (+); 31–50 %, positive (++); >50 %, strongly positive (+++). Sections were independently evaluated by two experienced pathologists blinded to the study. When the scores were different, a consensus was reached through consultation.

Extraction of total protein was performed using 200 mg of frozen tissues and the protein concentration was determined. The protein was stored at –70°C before use. Then, 20 μg of total protein thawed in 1 mL/mg lysis buffer containing protease inhibitors (1 % PBS, 1 % NP40, 0.5 % sodium deoxycholate, 0.1 % SDS, 10 mg/mL phenylmethylsulfonyl fluoride, 100 mmol/L sodium orthovanadate, protease inhibitors). The protein concentration was determined using a standard Lowry method. A human HIF-1α and VEGF-A DuoSet ELISA Development System (R&D) was used to quantify human HIF-1α and VEGF-A levels. Results were normalized to proteins.

The paraffin-embedded tissues were cut into sections and TUNEL assay was performed according to the manufacturer's instructions (Roche). TUNEL positive cells demonstrated karyopyknosis, chromatin aggregation and dark nucleus. Negative cells were blue and had a normal nucleus. A total of 20 fields were randomly selected from each section at a magnification of 400× and positive cells were counted followed by calculation of the apoptotic index (AI) as follows: AI = (number of positive cells/total number of cells) × 100 %.

Data were presented as mean and standard deviation. Statistical analyses were performed using SPSS 10.0 software. Statistical comparison of tumor volume, HIF-1α and VEGF-A expression, as well as numbers of apoptotic tumor cells between two different treatment groups, were made using t-tests.

Results

Glial fibrillary acidic protein expression and H&E staining: Immunohistochemistry for Glial fibrillary acidic protein revealed positive staining (brown granules) in a variety of cells suggesting glioma. H&E staining showed nuclear atypia and cell pleomorphism in tumor (Fig. 1).

Tumor volume and survival time: Tumor volume in the PDT group was markedly decreased compared to the control group. In the endostar group, cancer growth was significantly slower compared to the control group. In the PDT+endostar group, cancer growth was significantly slower than that of the PDT group or endostar group (Fig. 2).

Kaplan-Meier survival analysis showed that the mean survival was 17.100±1.120 days in control group, which was significantly shorter than that of the PDT group (31.700±1.647 days) or endostar group (24.900±1.464 days). The survival in the PDT+endostar group was the longest at 43.200±1.679 days (Fig. 3).

Detection of protein expression of HIF-1α and VEGF-A by ELISA: HIF-1α levels, measured by ELISA, in control group, PDT group, endostar group and PDT+endostar group was 223.56±22.39, 769.98±53.38, 109.24±35.21 and 369.87±36.94 pg/mg. VEGF-A levels, measured by ELISA, in control group, PDT group, endostar group and PDT+endostar group was 919.39±63.31, 1860.39±163.58, 369.87±63.35 and 1058.39±83.38 pg/mg.

HIF-1α and VEGF-A expression in the PDT group was markedly higher compared to the control group, but was lower in the endostar group compared to the control group. Moreover, VEGF-A expression in the PDT+endostar group was markedly lower compared to the PDT group (Fig. 4).

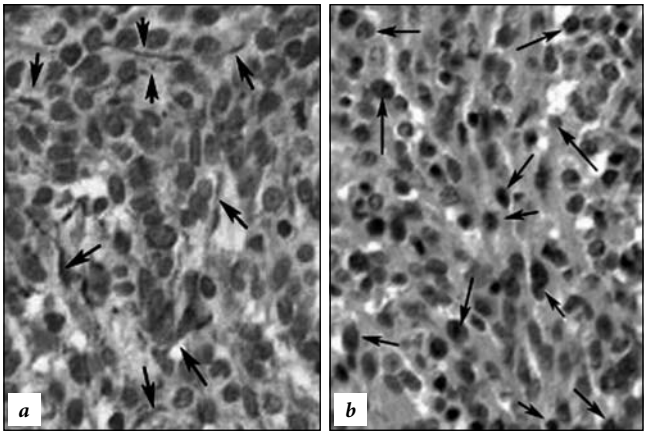

Figure 1. Glial fibrillary acidic protein expression:
a – the arrows show the GFAP positive cells; b – the arrows show the nuclear atypia. GFAP expression (a), H&E staining (b), ×400.

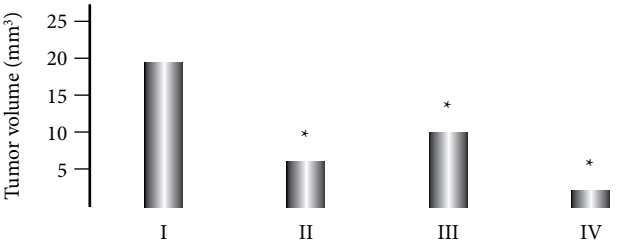

Figure 2. Tumor volume at 3 weeks after inoculation:
*I – control group, II – PDT group, III – endostar group, IV – PDT+endostar group; * p<0.05 compared the control group.*

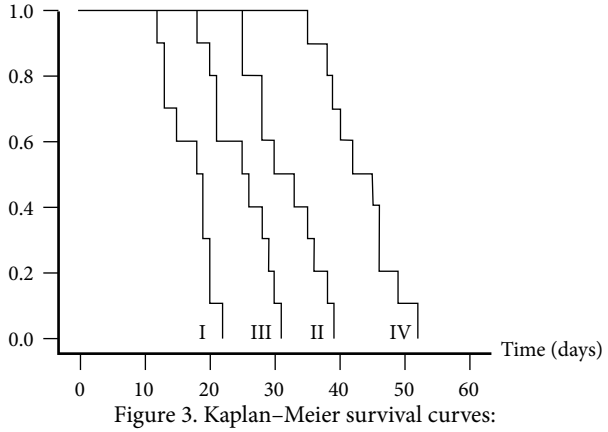

Figure 3. Kaplan–Meier survival curves:
I – control group, II – PDT group, III – endostar group, IV – PDT+endostar group.

Immunohistochemistry for HIF-1α and VEGF-A: HIF-1α positive cells had brown granules. HIF-1α was mainly expressed in the cytoplasm and nucleus of cancer cells. VEGF-A positive cells had yellow granules. VEGF-A was mainly expressed in the cytoplasm and membrane of cancer cells and endothelial cells. HIF-1α and VEGF-A expression in the PDT group was markedly higher compared to the control group, but was lower in the endostar group compared to the control group (Fig. 5, Fig. 6)

Apoptotic index: In the PDT group, endostar group and PDT+endostar group, TUNEL assay showed that some cells had shrinkage and chromatin margination

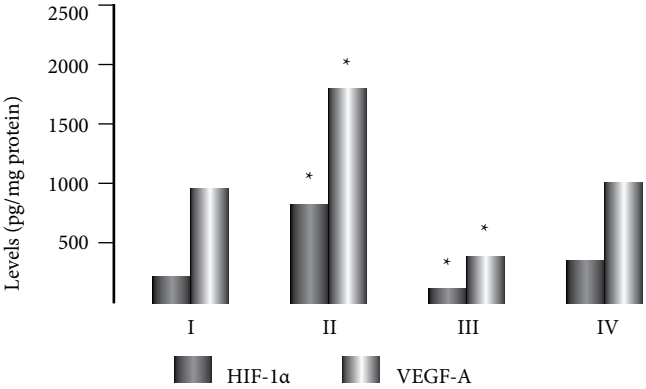

Figure 4. HIF-1α and VEGF-A protein expressions by ELISA:
*I – control group, II – PDT group, III – endostar group, IV – PDT+endostar group. Each group represents the mean of five individual tumor samples. Data are expressed as mean±SEM from two independent experiments. * p<0.05 compared the control group.*

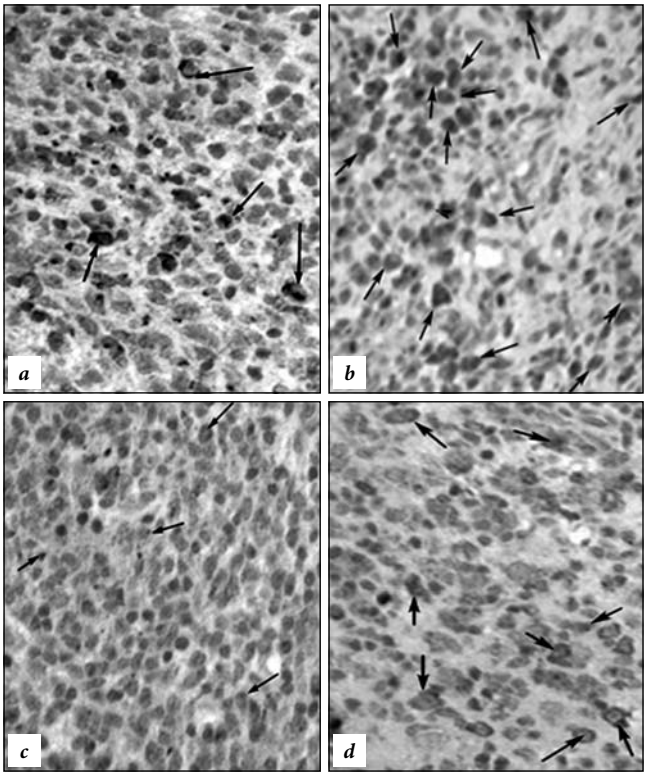

Figure 5. Immunohistochemistry for HIF-1α:
a – control group; b – PDT group; c – endostar group; d – PDT+endostar group. The arrows show the HIF-1α positive cells. ×400.

characterized by crescent shape or lobular shape. Apoptotic bodies were noted. The apoptotic index was 39.3±3.4, 25.4±2.8 and 61.7±4.9 % in the PDT group, endostar group and PDT+endostar group, respectively. In the control group, the cells had integral morphology and scant apoptotic cells. The apoptotic index in the control group was 7.8±0.5 % (Fig. 7).

Discussion

In the present study, we demonstrated that PDT combined with endostar significantly reduced tumor volume and prolonged survival time of nude mice bearing glioblastoma, compared with either no treatment or monotherapies .

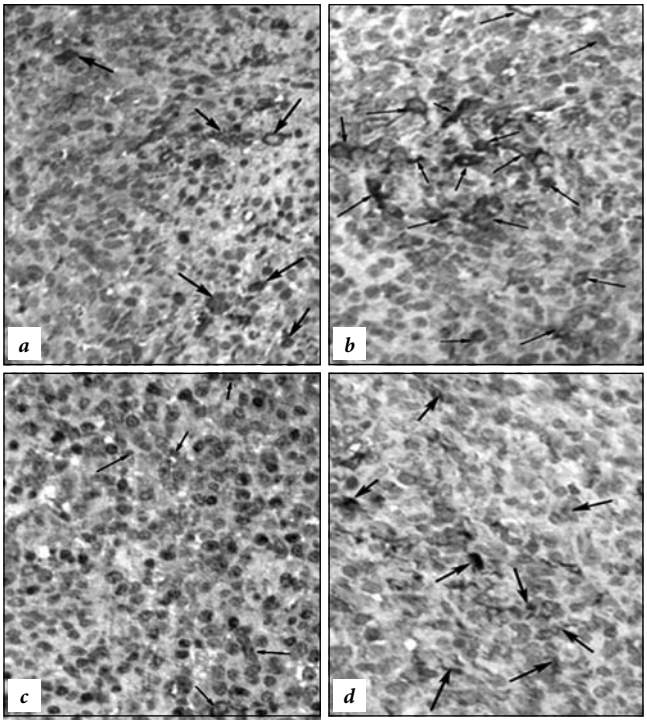

Figure 6. Immunohistochemistry for VEGF-A:
a – control group; b – PDT group; c – endostar group; d – PDT+endostar group. The arrows show the VEGF-A positive cells.

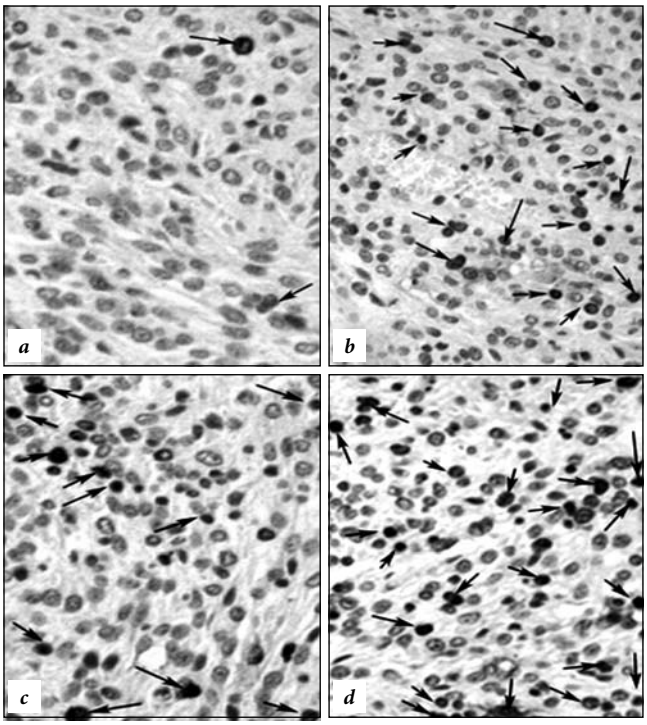

Figure 7. TUNEL assay:
a – control group; b – PDT group; c – endostar group; d – PDT+endostar group. The arrow shows apoptotic cells.

Hematoporphyrin monomethyl ether is a novel photosensitive reagent developed in China. *In vitro* and *in vivo* studies have shown that Hematoporphyrin monomethyl ether is a promising photosensitizer. S.S. Hu et al. [8] have shown, in their in vitro study, that Hematoporphyrin monomethyl ether mediated PDT could induce the

apoptosis of C6 cells and that calcium overload played an important role in extensive ultrastructural damage. In the present study, in the PDT group was significantly reduced tumor volume and prolonged survival time, which further confirmed that PDT can inhibit the growth of glioma in vivo. However, in the PDT group residual cancer cells highly expressed HIF-1α and VEGF-A, which is beneficial for angiogenesis. Thus, cancer cells can escape from the attack, resulting in the proliferation of residual cancer cells and subsequent recurrence and metastasis, which are the main cause of unfavorable long-term efficacy of PDT.

In 1970s, professor J. Folkman et al. first proposed the theory of antiangiogenic as an anti-tumor therapy [6]. In 1997, M.S. O›Reilly et al [12] found endostatin. Endostatin is considered as the most active inhibitor of angiogenesis. F.H. Barnett et al. [1] applied intra-arterial delivery of endostatin gene to 9L glioblastoma model prolongs survival and tumor volume reduction. N.O. Schmidt et al. [13] demonstrated that local i.c. administration of endostatin at a total daily dose of 2 mg/kg via osmotic minipumps inhibited the growth of intracranial U87 human glioblastoma xenografts in nude mice by 73.6 % and was associated with a decrease in blood vessel density and a significant increase in apoptosis. Our results showed that, in the endostar group was significantly reduced tumor volume . Endostar could inhibit not only the endogenous VEGF-A expression in normal U251 glioma cells but also the increased VEGF-A expression induced by photodynamic therapy.

In short, endostar in combination with PDT could markedly decrease PDT induced HIF-1α and VEGF-A expression, inhibiting new angiogenesis and simultaneously increase the apoptosis of cancer cells, which may be the primary way endostar enhances the efficacy of PDT in glioma. PDT, in combination with endostar, can more effectively prolong survival, and increase the apoptosis of cancer cells compared to either PDT or endostar alone. This finding may be a promising strategy in the treatment of malignant tumors.

Acknowledgement: This study was supported by the National Natural Science Foundation of China under grant (No. 30470586, 30872650) and Program for New Century Excellent Talents In University of Ministry of Education of China (NCET-09-0131).

References

1. Barnett F.H., Scharer-Schuksz M., Wood M. et al. Intra-arterial delivery of endostatin gene to brain tumors prolongs survival and alters tumor vessel ultrastructure // Gene Ther. 2004. Vol. 11. P. 1283–1289.
2. Bhuvaneswari R., Yuen G.Y., Chee S.K., Olivo M. Hypericin-mediated photodynamic therapy in combination with Avastin (bevacizumab) improves tumor response by downregulating angiogenic proteins // Photochem. Photobiol. Sci. 2007. Vol. 6. P. 1275–1283.
3. Candolfi M., Curtin J.F., Nichols W.S. et al. Intracranial glioblastoma models in preclinical neuro-oncology: neuropathological characterization and tumor progression // J. Neurooncol. 2007. Vol. 85. P. 133–148.
4. Chen Q., Huang Z., Chen H. et al. Improvement of tumor response by manipulation of tumor oxygenation during photodynamic therapy // Photochem. Photobiol. 2002. Vol. 76. P. 197–203.
5. Ferrario A., von Tiehl K.F., Rucker N. et al. Antiangiogenic treatment enhances photodynamic therapy responsiveness in a mouse mammary carcinoma // Cacer Res. 2000. Vol. 60. P. 4066–4069.
6. Folkman J. Anti-angiogenesis: new concept for therapy of solid tumors // Ann. Surg. 1972. Vol. 175. P. 409–416.
7. Forsythe J.A., Jiang B.H., Iyer N.V. et al. Activation of vascular endothelial growth factor gene transcription by hypoxia-inducible factor 1 // Mol. Cell. Biol. 1996. Vol. 16. P. 4604–4613.
8. Hu S.S., Cheng H.B., Zheng Y.R. et al. Effects of photodynamic therapy on the ultrastructure of glioma cells // Biomed. Environ. Sci. 2007. Vol. 20. P. 269–273.
9. Huita W.U., Jie Deng, Shiying Y.U. et al. The inhibitory effects of Rh-endostatin (YH-16) in combination with radiotherapy on lung adenocarcinoma A549 in mice and the underlying mechanisms // J. Huazhong. Univ. Sci. Technol. 2010. Vol. 30. P. 108–112.
10. Jin F., Gao C., Zhao L. et al. Using CD133 positive U251 glioblastoma stem cells to establish nude mice model of transplanted tumor // Brain Res. 2011. Vol. 1368. P. 82–90.
11. Madsen S.J., Kharkhuu K. Hirschberg H. Utility of the F98 rat glioma model for photodynamic therapy // J. Environ. Pathol. Toxicol. Oncol. 2007. Vol. 26. P. 149–155.
12. O'Reilly M.S., Boehm T., Shing Y. et al. Endostatin: an endogenous inhibitor of angiogenesis and tumor growth // Cell. 1997. Vol. 88. P. 277–285.
13. Schmidt N.O., Ziu M., Carrabba G. et al. Antiangiogenic therapy by local intracerebral microinfusion improves treatment efficiency and survival in an orthotopic human glioblastoma model // Clin. Cancer Res. 2004. Vol. 10. P. 1255–1262.
14. Smith J.S., Chang E.F., Lamborn K.R. et al. Role of extent of resection in the long-term outcome of low-grade hemispheric gliomas // J. Clin. Onco. 2008. Vol. l26. P. 1338–1345.
15. Zhou Q., Olivo M., Lye K.Y. et al. Enhancing the therapeutic responsiveness of photodynamic therapy with the antiangiogenic agents SU5416 and SU6668 in murine nasopharyngeal carcinoma models // Cancer Chemother. Pharmacol. 2005. Vol. 56. P. 569–577.

Поступила в редакцию 24.06.2013.

ЭФФЕКТИВНОСТЬ ФОТОДИНАМИЧЕСКОЙ ТЕРАПИИ И РЕКОМБИНАНТНОГО ЧЕЛОВЕЧЕСКОГО ЭНДОСТАТИНА В УГНЕТЕНИИ РОСТА ПЕРЕВИВАЕМОЙ ГЛИОМЫ U251 *IN VIVO*

Ху Шаошан[1], *Жан Кви*[2], *Юе Ву*[2]
[1] *Отделение нейрохирургии Второго аффилированного госпиталя,* [2] *Отделение нейрохирургии Четвертого аффилированного госпиталя Харбинского медицинского университета (КНР, 150081, г. Харбин, р-н Наньган, шоссе Баоян, 157)*

Endostar – новый рекомбинантный человеческий эндостатин, полученный в системе экспрессии *Escherichia coli*, был разрешен SFDA к использованию на территории Китая. Для изучения эффективности Endostar и фотодинамической терапии (ФДТ) бестимусных мышей с перевиваемой глиомой U251 разделили на 4 группы: «ФДТ+Endostar», «ФДТ», «Endostar» и «Контроль». В группе «ФДТ» пролонгированная по сравнению с контролем выживаемость сопровождалась усилением апоптоза клеток опухоли. При сочетании ФДТ и эндостатина данные изменения были выражены сильнее. После ФТД заметно усиливалась экспрессия индуцируемого при гипоксии фактора-1-альфа (HIF-1α) и фактора роста эндотелия сосудов А (VEGF-A), а после лечения эндостатином экспрессия этих факторов значимо снижалась. Таким образом, ФДТ в сочетании с эндостатином эффективно угнетает рост перевиваемой глиомы U251. Подобный подход может быть эффективен при разработке стратегии лечения злокачественных опухолей.

Ключевые слова: *злокачественные опухоли, Endostar, индуцируемый при гипоксии фактор, фактор роста эндотелия сосудов.*